Role of zooplankton in determining the efficiency of the biological carbon pump

Cavan, Emma. L. [1*], Henson, Stephanie. A. [2], Belcher, Anna. [1] & Sanders, Richard. [2]

[1]University of Southampton, National Oceanography Centre, European Way, Southampton, SO14 3ZH, UK

[2]National Oceanography Centre, European Way, Southampton, SO14 3ZH, UK.

*Corresponding author: Emma L. Cavan, University of Southampton, National Oceanography Centre, European Way, Southampton, SO14 3ZH, UK. (+44) 2380 598724. e.cavan@noc.soton.ac.uk.

Abstract

The efficiency of the ocean's biological carbon pump (BCP*eff* – here the product of particle export and transfer efficiencies) plays a key role in the air-sea partitioning of CO_2. Despite its importance in the global carbon cycle, the biological processes that control BCP*eff* are poorly known. We investigate the potential role that zooplankton play in the biological carbon pump using both *in situ* observations and model output. Observed and modelled estimates of fast, slow and total sinking fluxes are presented from three oceanic sites: the Atlantic sector of the Southern Ocean, the temperate North Atlantic and the equatorial Pacific oxygen minimum zone (OMZ). We find that observed particle export efficiency is inversely related to primary production likely due to zooplankton grazing, in direct contrast to the model estimates. The model and observations show strongest agreement in remineralization coefficients and BCP*eff* at the OMZ site where zooplankton processing of particles in the mesopelagic zone is thought to be low. As the model has limited representation of zooplankton-mediated remineralization processes, we suggest that these results point to the importance of zooplankton in setting BCP*eff*, including particle grazing and fragmentation, and the effect of diel vertical migration. We suggest that improving parameterizations of zooplankton processes may increase the fidelity of biogeochemical model estimates of the biological carbon pump. Future changes in climate such as the expansion of OMZs may decrease the role of zooplankton in the biological carbon pump globally, hence increasing its efficiency.

Keywords

Biological carbon pump, zooplankton, remineralization

1. Introduction

The biological carbon pump plays an important role in regulating atmospheric carbon dioxide levels (Kwon et al., 2009; Parekh et al., 2006). Phytoplankton in the surface ocean convert inorganic carbon during photosynthesis to particulate organic carbon (POC), a fraction of which is then exported out of the upper ocean. As particles sink through the interior ocean they are subject to remineralization by heterotrophs, such that only a small proportion of surface produced POC reaches the deep ocean (Martin et al. 1987). The efficiency of the biological carbon pump (BCP*eff*; defined here as the proportion of surface primary production that is transferred to the deep ocean (Buesseler and Boyd, 2009) therefore affects the air-sea partitioning of CO_2 (Kwon et al., 2009). Greater understanding on the controls of this term may consequently result in more accurate assessments of the BCP's role in the global carbon cycle.

One approach to determine BCP*eff* over long time scales (millennia) is by assessing the relative proportions of preformed and regenerated nutrients, i.e. the fraction of upwelled nutrients that is removed from surface waters by biological uptake (Hilting et al., 2008). However to assess BCP*eff* over much shorter timescales (days to weeks) we use the definition of Buesseler & Boyd (2009) where BCP*eff* is the product of particle export efficiency (PE*eff*, the ratio of exported flux to mixed layer primary production) and transfer efficiency (T*eff*, the ratio of deep flux to exported flux). Using these two parameters together allows a more in-depth analysis of the biological processes involved and thus the assessment of the role of zooplankton in setting BCP*eff*. Additionally the attenuation coefficients Martin's *b* (Martin et al. 1987) and the remineralization length scale z^* (Boyd and Trull,

2007) are useful to quantify how rapidly exported POC is remineralized in the mesopelagic zone.

PE*eff* varies proportionally to primary production, although uncertainty exists as to whether the relationship is inverse or positive (Aksnes and Wassmann, 1993; Cavan et al., 2015; Henson et al., 2015; Laws et al., 2000; Maiti et al., 2013; Le Moigne et al., 2016). Potential controls on PE*eff* include temperature (Henson et al., 2015; Laws et al., 2000), zooplankton grazing (Cavan et al., 2015), microbial cycling (Le Moigne et al., 2016), mineral ballasting (Armstrong et al., 2002; François et al., 2002; Le Moigne et al., 2012) or large export of dissolved organic carbon (Maiti et al., 2013). T*eff* and POC attenuation coefficients describe how much of the exported POC reaches the deep ocean and how much of it is remineralized. Essentially the attenuation of POC with depth is determined by the sinking rates of particles and how rapidly the POC is turned over (Boyd and Trull, 2007). However, these factors themselves are controlled by various other processes such as: ballasting by minerals (François et al., 2002; Le Moigne et al., 2012), epipelagic community structure (Lam et al., 2011), temperature (Marsay et al., 2015), lability of the particles (Keil et al., 2016) and zooplankton diel vertical migration (Cavan et al., 2015). Therefore it is unlikely that any single factor controls BCP*eff*.

The role of zooplankton in controlling the efficiency of the BCP is often overlooked, with greater focus on factors such as biominerals for ballasting (De La Rocha and Passow, 2007) or microbial respiration (Herndl and Reinthaler, 2013). Nevertheless zooplankton have the potential to significantly impact the biological carbon pump as they can consume and completely transform particles (Lampitt et al., 1990). Grazing by zooplankton results in POC either passing through the gut and being egested as a fecal pellet, being respired as CO_2 or

97 fragmented into smaller particles through sloppy feeding (Lampitt et al., 1990). Further,
98 zooplankton can undergo diel vertical migration, feeding on particles at night in the surface
99 and egesting them at depth during the day (Wilson et al., 2013). Consequently a significant
100 proportion of POC may escape remineralization in the upper mesopelagic zone (Cavan et al.,
101 2015), where recycling of POC is most intense (Martin et al. 1987).
102
103 In this study we combine observations (made using Marine Snow Catchers, MSCs) and
104 model output to investigate the role of zooplankton in setting the efficiency of the biological
105 carbon pump in three different oceanic regions: the Atlantic sector of the Southern Ocean
106 (SO), the Porcupine Abyssal Plain (PAP) site in the temperate North Atlantic and the
107 Equatorial Tropical North Pacific (ETNP) oxygen minimum zone. The ecosystem model
108 used here, MEDUSA (Yool et al., 2013), was chosen as it separates particle fluxes into slow
109 and fast sinking groups. Additionally the only interactions of zooplankton with particles in
110 MEDUSA are through the production of particles (fecal pellets) and by grazing on slow
111 sinking particles only. Here we compare various indices of BCP*eff* between the observations
112 and model to infer the role of zooplankton in controlling BCP*eff*.
113
114 **2. Methods**
115 **2.1 Site description**
116 Three very different sites were chosen in this study: the Atlantic sector of the Southern Ocean
117 Ocean (SO, 45 – 65 °S, 20 – 70 °W), the Porcupine Abyssal Plain (PAP) site in the temperate
118 North Atlantic (49 °N, 17 °W) and the Equatorial Tropical North Pacific (ETNP) oxygen
119 minimum zone (13 °N, 91 °W) (Fig. 1). The SO accounts for ~ 20 % of the global ocean CO_2
120 uptake (Park et al., 2010; Takahashi et al., 2002) and is a large high-nutrient-low-chlorophyll
121 region, in part due to limited iron availability (Martin, 1990). Nevertheless, iron from oceanic

122 islands and melting sea ice can cause intense phytoplankton blooms, which may lead to high
123 POC export (Pollard et al., 2009). In the temperate North Atlantic seasonality is high, with
124 phytoplankton blooms occurring in spring and summer (Lampitt et al., 2001). The region
125 contributes disproportionally to global export, accounting for 5 – 18 % of the annual global
126 export (Sanders et al., 2014). In the ETNP region a strong oxygen minimum (OMZ) persists
127 where, between 50 and 1000 m depth, dissolved oxygen concentration can fall below 2 μmol
128 kg^{-1} (Paulmier and Ruiz-Pino, 2009). In OMZs the low oxygen concentrations may lead to a
129 high transfer efficiency of POC flux potentially due to reduced heterotrophy (Devol and
130 Hartnett, 2001; Hartnett et al., 1998; Keil et al., 2016; Van Mooy et al., 2002).
131
132 **2.2 Observations**
133 Particles were collected using Marine Snow Catchers (MSCs) (Riley et al., 2012) from the
134 three oceanic sites as shown in Fig. 1. In total 27 stations were sampled, 18 in the SO, 5 at
135 PAP and 4 in the ETNP (Table S1). MSCs have the advantage of being able to separate
136 particles intact into two groups dependent on their sinking rate, fast (> 20 m d^{-1}) or slow (<
137 20 m d^{-1}). MSCs were deployed below the mixed layer depth (MLD), which was determined
138 as the depth with the steepest gradient of salinity and temperature, and usually occurred
139 between 20 and 70 m (Table S1). The shallowest MSC was deployed 10 m below the MLD
140 and another 100 m deeper than this for the Southern Ocean (Cavan et al., 2015) and the PAP
141 site. In the ETNP MSCs were also deployed deeper into the water column to a maximum
142 depth of 220 m.
143
144 Fast and slow sinking particles were collected from the MSC following the protocol by Riley
145 et al. (Riley et al., 2012). Images of fast sinking particles were taken to estimate the
146 equivalent spherical diameter (ESD) of the particles and ESD converted to POC mass *via*

147 conversion factors, CFs (Alldredge, 1998; Cavan et al., 2015). Two different CFs were used,
148 one for phytodetrital aggregates (PDAs, Eq 1) and one for faecal pellets (FPs, Eq 2):

149 Phytodetrital aggregates $m = 1.09 * V^{0.52}$ (Equation 1)

150 Faecal pellets $m = 1.05 * V^{0.51}$ (Equation 2)

151 where m is mass of POC and V volume of the particle. Very few published studies exist
152 comparing size of particles to carbon content, and those that do tend to focus on FPs (Manno
153 et al., 2015). We chose to use the Alldredge (1998) CF because it allows comparison with
154 other published studies (e.g. Ebersbach and Trull, 2008; Guidi et al., 2007; Laurenceau et al.,
155 2015; Riley et al., 2012, Belcher et al., 2016), describes the fractal nature of particles and is
156 an upper ocean study (50 % of our observations lie close to the depth (~20 m) of the
157 Alldredge (1998) particles; Table S1). Another important point is that the MSCs allow
158 collection of particles relatively undamaged or unaltered compared to sediment traps (other
159 than gel traps), making the use of conversion factors more reliable as particle shapes reflect
160 those measured *in situ* (Romero-Ibarra and Silverberg, 2011).
161
162 To test the robustness of the Alldredge (1998) CFs we compared the resulting POC mass with
163 that calculated using the CFs from Manno et al. (2015). This study was done in the Southern
164 Ocean and only focussed on FPs, hence we only tested the similarity using our SO data where
165 FPs comprised most (> 60 %) of the particle flux (Fig. S1). Manno et al. found a linear
166 relationship between FP size and POC content for cylindrical FPs (0.018 mg C mm^{-3}). We
167 calculated the total fast sinking POC mass (FP + PDA) using the Manno CF for FPs and
168 Alldredge CFs for the PDAs (remembering that FPs dominated flux) and compared these to
169 just using the Alldredge CFs (Fig. S2 a). The slope of the regression between the two is very
170 close to 1 at 0.96 showing neither CF under- or over estimates POC relative to the other.
171 There was no statistical difference (t-test, t = 0.25, df = 77.23, p-value = 0.80) between the

mean masses of the two methods, with Manno CFs producing a mean mass of POC per sample of 11 µg C and Alldredge CFs producing a mean of 8.4 µg C. Therefore we conclude that using the Alldredge CFs is justified and using one general CF allows comparisons between our different study regions.

Slow sinking and suspended particles were filtered onto ashed (400 °C, overnight) GF/F filters and run in a HNC elemental analyser to determine POC mass. Sinking rates were estimated for fast sinking particles in the SO and at PAP by placing particles into a measuring cylinder filled with *in situ* sea water and timing how long it took each particle to pass a discrete point (Cavan et al., 2015). At the ETNP a FlowCAM was used to measure fast particle sinking rates (Bach et al., 2012). All slow sinking particle rates were calculated using the SETCOL method (Bienfang, 1981). Fluxes (mg C m^{-2} d^{-1}) were calculated by dividing the mass of POC (mg) by the area of the MSCs (m^2) and the sinking time of the particles (d) (Cavan et al., 2015). Primary production (PP) was estimated from 8-day satellite-derived data using the Vertically Generalised Productivity Model (Behrenfeld and Falkowski, 1997) applied to MODIS data.

2.3 Model output

The ecosystem model MEDUSA (Yool et al., 2013) was used for this study as it distinguishes detrital fluxes in two pools, fast and slow sinking. In MEDUSA, fast sinking particles are assumed to sink more rapidly than the time-step of the model and are remineralized instantaneously at all vertical levels with the flux profile determined by a ballast model (Armstrong et al., 2002). Slow sinking particles sink at 3 m d^{-1} and remineralization is temperature dependent, with zooplankton grazing on slow sinking particles but not on the fast sinking particles. Zooplankton DVM is not parameterised. Primary production is modelled as

197 non-diatom and diatom production, which is summed to give the total depth-integrated
198 primary production. The model was run in hindcast mode at ¼ ° spatial resolution and output
199 saved with a 5-day temporal resolution. The model output was extracted at the same locations
200 and times as the observations were made and averaged over 12 years (1994 - 2006) to give
201 the climatological seasonal cycle. The model outputs fluxes of particulate organic nitrogen
202 (mg N m^{-2} d^{-1}) which are converted to POC (mg C m^{-2} d^{-1}) using the Redfield ratio (Redfield,
203 1934).
204
205 **2.4 Data manipulation**
206 For both the observations and the model output the fast and slow sinking fluxes were
207 summed to calculate the total sinking POC flux. Model output was available at fixed depths
208 of 100 and 200 m, which introduces an offset with our at-sea observations (Table S1). This
209 study is therefore assessing BCP*eff* in the upper ocean only. Parameters calculated to test the
210 efficiency of the biological carbon pump were the percentage contribution of fast and slow
211 sinking particles to the total sinking flux, particle export efficiency (PE*eff*), the attenuation of
212 flux with depth expressed as *b* and *z** and transfer efficiency (T*eff*).
213
214 PE*eff* is the proportion of surface produced primary production (PP) that is exported out of
215 the mixed layer (observations) or at 100 m (model) and is calculated by dividing the exported
216 flux by PP. To estimate the attenuation of flux over the upper mesopelagic zone the
217 exponents *b* (Martin et al. 1987) and *z** (Buesseler and Boyd, 2009) were calculated, where
218 fluxes at the export depth and 100 m below were used for observations and fluxes at 100 and
219 200 m from the model. The *b* exponent is dimensionless and generally ranges from 0 to 1.5
220 with low values indicating low attenuation, thus low remineralization, and higher values
221 representing high attenuation and remineralization. The *z** (m) exponent is the

remineralization length scale, or the depth by which only 37 % of the reference flux (here at the export depth) remains. Thus a large z^* suggests low attenuation and low remineralization of the particle flux. The T*eff* is another parameter that represents how much flux reaches the deeper ocean and hence is not remineralized. This is simply calculated by dividing the deep flux (125 – 220 m in observations and 200 m in model) by the export flux. All indices are dimensionless apart from z^* which is in metres.

3. Results and Discussion

3.1 Comparison of fluxes

We compare model output with satellite-derived estimates of primary production (PP), POC export and deep (150 - 300 m) fluxes in the upper ocean (Fig. S3). Overall, modelled PP compares well compared to satellite-derived estimates with a strong positive correlation between the two ($p < 0.001$, $r^2 = 0.84$, Fig. S3 a), although the model slightly overestimates PP. When comparing the total sinking export fluxes and total deep fluxes, most points lie below the 1:1 line, suggesting that the model is overestimating POC flux (Figs. S3 b & c).

3.2 Observed particles

In all three regions particles were classified as phytodetrital aggregates (PDAs) or faecal pellets (FPs) using the images taken. PDAs were of a similar aesthetic nature in all three areas (Fig. 2) consisting of unidentifiable (to phytoplankton species level) detrital material. In the SO FPs were either from krill which form long chains of pellets (Fig. 2b) or copepods (Wilson et al., 2008). At PAP and in the ETNP, only copepod FPs were observed (Fig. 2 d & f).

3.3 Export production

247 The traditional view of export production is that as PP increases, so does POC export out of
248 the mixed layer (Laws et al., 2000). However recent analyses from the Southern Ocean (SO)
249 observe the opposite relationship, that an inverse relationship between PE*eff* and PP exists
250 (Cavan et al., 2015; Maiti et al., 2013; Le Moigne et al., 2016). We find that for fast sinking
251 particles the model shows PE*eff* increases with PP (Fig. 3 a) according to a power law
252 function ($p < 0.001$, $r^2 = 0.6$) while the observations show an inverse relationship (logarithmic
253 function, $p < 0.001$, $r^2 = 0.4$), even when including sites outside of the SO. This inverse
254 relationship was preserved for the SO when including conversion factors of Manno et al.
255 (2015) (Fig. S2b).
256
257 However for the slow sinking particles the model shows an inverse relationship between PP
258 and PE*eff*, similar to that seen in the observations for the fast sinking particles (power law
259 function, $p<0.001$, $r^2=0.97$, Fig. 3 b). Potential reasons for an inverse relationship between PP
260 and *PEeff* include the temporal decoupling between primary production and export (Salter et
261 al., 2007), seasonal dynamics of the zooplankton community (Tarling et al., 2004) or grazing
262 by zooplankton (Cavan et al., 2015; Maiti et al., 2013; Le Moigne et al., 2016). As previously
263 mentioned one of the differences between the fast and slow sinking detrital pools in the
264 model is that slow sinking particles are grazed on by zooplankton and fast sinking are not.
265 Thus when zooplankton graze on particles in the model an inverse relationship between *PEeff*
266 and PP exists and when zooplankton grazing is not accounted for, the opposite occurs. This
267 highlights the importance of zooplankton in determining the efficiency of the BCP.
268
269 The observed slow sinking PE*eff* were generally very low (< 0.05) and thus had little
270 influence on the PE*eff* for total sinking POC flux, which also had a non-linear inverse
271 relationship with PP ($p < 0.001$, $r^2 = 0.4$, Fig. 3 c). It is important to note that high values of

PP (> 1000 mg C m^{-2} d^{-1}) were only present at PAP, and that the SO had the greatest range of PP, so drives a large part of the inverse relationship. Therefore measuring PE*eff* in other regions with large PP ranges is fundamental to see if this relationship holds outside the sites from this study.

3.4 Contribution of fast and slow sinking POC fluxes

Particles naturally sink at different rates, with one operational definition being that slow sinking particles sink at < 20 m d^{-1} and fast sinking particles at > 20 m d^{-1} (Riley et al., 2012). Most sediment traps cannot separately measure fluxes of fast and slow sinking particles and are unlikely to capture much of the slow sinking flux due to their deployment in the lower mesopelagic and bathypelagic zones (Buesseler et al., 2007; Lampitt et al., 2008). Slow sinking particles may sink too slowly and be remineralized too quickly to reach the deep ocean unless they are formed there. Hence the MSC is a useful tool to analyse the two sinking fluxes separately.

In both the model and the observations, the slow sinking flux was consistently smaller than the fast sinking flux and generally only contributed < 40 % of the total flux (Fig. S4). However in the model the proportion of slow sinking flux always decreases with depth (Figs. S4 a-c) whereas observations at the PAP site showed the proportion of slow sinking fluxes increased with depth (Figs. S4 e). Increases in slow sinking particles with depth must be from the fragmentation of larger fast sinking particles either abiotically (Alldredge et al., 1990) or from sloppy feeding by zooplankton (Lampitt et al., 1990) or advection or mixing (Dall'Olmo et al., 2016). Sloppy feeding results in zooplankton fragmenting particles into smaller particles resulting in a larger surface area to volume ratio increasing colonization by microbes and thus remineralization (Mayor et al., 2014). Zooplankton do not graze on fast

297 sinking particles in the model hence neither sloppy feeding nor abiotic fragmentation are
298 represented (Yool et al., 2013). This likely explains why the contribution of slow sinking
299 particles can only decrease with depth in the model, unlike the observations in which slow
300 sinking particles may increase with depth.
301
302 **3.5 Attenuation of POC with depth**
303 The attenuation of POC through the water column describes how quickly POC fluxes are
304 remineralized, with a high attenuation indicating high POC remineralization. We used the
305 parameters *b* (Martin et al. 1987) and *z** (Boyd and Trull, 2007) to describe the attenuation of
306 flux with depth. A recent study suggests POC remineralization is temperature dependent
307 (Marsay et al., 2015) hence we compared the attenuation coefficients with temperature.
308 Calculated mean *b* and *z** values for total (fast + slow) sinking POC from the model were
309 similar at all sites (Figs. 4 a & b) with no correspondence with temperature, even though slow
310 sinking particles are remineralized as a function of temperature in the model. Hence slow
311 sinking *b* and *z** increase and decrease respectively with temperature (Table S2). The
312 observations (for total sinking particles) show a non-linear relationship with temperature that
313 deviates away from the Marsay et al. (2015) regression, such that remineralization increases
314 (high attenuation) at temperatures greater than 13 °C. The variability is much greater in the
315 observations than the model, a feature that is consistent across all indices (Figs. 4 a & b).
316 Apart from at the ETNP where the model and observations agree, the observations
317 consistently show slower POC attenuation compared to the model. The active transfer of
318 POC to depth *via* diel vertical migration (DVM) of zooplankton (Wilson et al., 2008) may
319 contribute to the observed slower rates of POC attenuation. Cavan et al. 2015 showed that
320 high Southern Ocean *b* values were a result of DVM, a process not parameterized in the
321 MEDUSA model. Although active transfer *via* DVM is a complex process that may be

322 difficult to model, it is potentially important to include in biogeochemical models, as it has
323 been shown to account for 27 % of the total flux in the North Atlantic (Hansen and Visser,
324 2016).
325
326 The strong alignment of the modelled and observed attenuation at the ETNP is likely because
327 of the lack of particle processing by zooplankton, by design in the model and naturally in
328 oxygen minimum zones (OMZs). The daytime depth of vertically migrating zooplankton is
329 reduced in OMZs due to low dissolved oxygen concentrations (Bianchi et al., 2013), which at
330 the ETNP reach < 2 μmol kg^{-1} by 120 m. Further the population of zooplankton below this
331 depth is almost non-existent in OMZs (Wishner et al., 2013) and those that are there feed on
332 particles at the surface, not in the OMZ core (Williams et al., 2014). Thus zooplankton
333 consumption and manipulation of particles is greatly reduced in OMZs and is non-existent in
334 the MEDUSA model.
335
336 **3.6 Efficiency of the biological carbon pump**
337 To calculate BCP*eff* (proportion of mixed layer primary production found at depth, here 150 -
338 300 m) we replicated the BCP*eff* plots of Buesseler & Boyd (2009) by plotting PE*eff* against
339 transfer efficiency (T*eff*) for fast, slow and total sinking particles (Fig. 5). According to the
340 observations, the SO had the highest total sinking BCP*eff* at 40 %, similar to the maximum
341 observed by Buesseler & Boyd (2009) in the North Atlantic. The SO observations showed a
342 higher BCP*eff* than the model by about 10 % across all sinking fluxes (Fig. 5). This
343 difference was largely due to a very high T*eff* (> 1) estimated from observations, which
344 implies fluxes increased at depth. This could be due to active fluxes by vertically migrating
345 zooplankton, possibly krill (Cavan et al., 2015). Active fluxes could account for high

346 observed T*eff* in the slow sinking particles, as well as fragmentation of larger particles at
347 depth (Mayor et al., 2014).
348
349 T*eff* is often thought to be controlled by the dominant phytoplankton group in the upper
350 ocean, which is linked to the ballasting hypothesis (Francois et al., 2002; Henson et al.,
351 2012). T*eff* for total POC flux estimated by the model (Fig. 5 c) is roughly the same in all
352 three regions, even though the MEDUSA model is capable of altering the ratio of diatom to
353 non-diatom PP (Yool et al., 2013), as would be expected when comparing the Southern
354 Ocean and the Equatorial Pacific. Diatoms often dominate the SO (Salter et al., 2007) whilst
355 the ETNP is dominated by pico- and nanophytoplankton (Puigcorbé et al., 2015), and at the
356 PAP site a range of phytoplankton species are found from diatoms to smaller cyanobacteria
357 and dinoflagellates (Smythe-Wright et al., 2010).
358
359 In this study we observe the opposite trend in T*eff* compared to Henson et al. (2012) with the
360 SO exhibiting high T*eff* (> 1) and the ETNP the lowest (~ 0.5). This could be due to the depth
361 range over which T*eff* is calculated as here it is relatively shallow (< 200 m) compared to the
362 2000 m range in Henson et al. (2012). For instance, Henson et al. (2012) estimate T*eff* of ~
363 0.4 in the ETNP, very close to the calculated values in this study, which due to the
364 hypothesised lack of zooplankton interactions with particles in the deep OMZs could remain
365 unchanged if calculated at 2000 m depth. However, in the SO zooplankton influence particle
366 transfer heavily and thus if we had observed T*eff* at 2000 m, it may have been much lower,
367 and conform to the finding that at high latitudes PE*eff* is high and T*eff* is low (Henson et al.,
368 2012). This highlights the potential complex interactions between particles and zooplankton
369 in the upper mesopelagic zone which may be missed in deep ocean particle studies.
370

371 Even though the PAP site had the highest PP, the BCP*eff* was lowest (< 15 %). There were
372 also large differences (up to 15 %) in the BCP*eff* between the model and the observations at
373 the PAP site driven by large discrepancies in PE*eff*. Observations of fast sinking PE*eff* were
374 much lower than predicted by the model (Fig. 5 a), which we suggest could result from active
375 grazing and fragmentation of fast sinking particles by zooplankton. T*eff* of fast sinking
376 particles was low and consistent with model predictions, suggesting that active transfer via
377 DVM (not parameterized in the model) plays a relatively minor role at the PAP site.
378 Therefore mineral ballasting (Armstrong et al., 2002), which drives T*eff* in the model, may be
379 the main driver of T*eff* at PAP. The modelled and observed slow sinking BCP*eff* were similar
380 at PAP (~ 1 %) despite a large difference in T*eff* (Fig. 5 b). Fragmentation of fast to slow
381 sinking particles (not included in the model) at depth could explain the difference in slow
382 sinking T*eff*.
383
384 Finally the BCP*eff* for the ETNP is very similar between the model and observations for all
385 sinking fluxes (Fig. 5). The similarity in the BCP*eff* here echoes the similarity shown for
386 POC attenuation with depth. This reiterates our hypothesis that the model and observations
387 agree on BCP*eff* only in areas of the global ocean where processing of particles by
388 zooplankton is reduced due to very low dissolved oxygen concentrations.
389
390 **4. Conclusions**
391 We have used observations and model output from the upper mesopelagic zone in 3
392 contrasting oceanic regions to assess the influence of zooplankton on the efficiency of the
393 biological carbon pump. We separately collected *in situ* fast and slow sinking particles, which
394 are also separated into discrete classes in the MEDUSA model. The model has limited

processing of particles by zooplankton with only slow sinking detrital POC being grazed upon.

Our results highlight the crucial role that zooplankton play in regulating the efficiency of the biological carbon pump through 1) controlling particle export by grazing, 2) fragmenting large, fast sinking particles into smaller, slower sinking particles and 3) active transfer of POC to depth *via* diel vertical migration. Comparisons of the model and observations in an oxygen minimum zone provide strong evidence of the importance of zooplankton in regulating the BCP. Here extremely low dissolved oxygen concentrations at depth reduce the abundance and metabolism of zooplankton in the mid-water column. Thus the ability of zooplankton to degrade or repackage particles is vastly reduced in OMZs, and as such it is here that the model, with limited zooplankton interaction with particles, shows the strongest agreement with observations.

We recommend that grazing on large, fast sinking particles and the fragmentation of fast to slow sinking particles (either *via* zooplankton or abiotically) is introduced into global biogeochemical models, with the aim of also incorporating active transfer. Future changes in climate such as the expansion of OMZs may decrease the role of zooplankton in the biological carbon pump globally, increasing its efficiency and hence forming a positive climate feedback.

Acknowledgements

We would like to thank all participants and crew on cruises JR274, JC087, JC097. Thanks to Annike Moje for running all POC samples in Bremen, Germany. Thanks also to Andrew Yool for providing the MEDUSA model output.

420

421 **References**

422

423 Aksnes, D. and Wassmann, P.: Modeling the significance of zooplankton grazing for export
424 production, Limnol. Oceanogr., 38(5), 978–985, 1993.
425 Alldredge, A.: The carbon, nitrogen and mass content of marine snow as a function of
426 aggregate size, Deep. Res. I, 45(4-5), 529–541, 1998.
427 Alldredge, A., Granata, T. C., Gotschalk, C. C. and Dickey, T. D.: The physical strength of
428 marine snow and its implications for particle disaggregation in the ocean, Limnol. Oceanogr.,
429 35(November), 1415–1428, doi:10.4319/lo.1990.35.7.1415, 1990.
430 Armstrong, R., Lee, C., Hedges, J., Honjo, S. and Wakeham, S.: A new, mechanistic model
431 for organic carbon fluxes in the ocean based on the quantitative association of POC with
432 ballast minerals, Deep. Res. II, 49(1-3), 219–236, 2002.
433 Bach, L. T., Riebesell, U., Sett, S., Febiri, S., Rzepka, P. and Schulz, K. G.: An approach for
434 particle sinking velocity measurements in the 3-400 μm size range and considerations on the
435 effect of temperature on sinking rates., Mar. Biol., 159(8), 1853–1864, doi:10.1007/s00227-
436 012-1945-2, 2012.
437 Behrenfeld, M. J. and Falkowski, P. G.: Photosynthetic rates derived from satellite-based
438 chlorophyll concentration, Limnol. Oceanogr., 42(1), 1–20, 1997.
439 Belcher, A., Iversen, M. H., Manno, C., Henson, S. A., Tarling, G. A. and Sanders, R.: The
440 role of particle associated microbes in remineralisation of faecal pellets in the upper
441 mesopelagic of the Scotia Sea, Antarctica, Limnol. Oceanogr., 61, 1049–1064,
442 doi:10.1002/lno.10269, 2016.
443 Bianchi, D., Stock, C., Galbraith, E. D. and Sarmiento, J. L.: Diel vertical migration :
444 Ecological controls and impacts on the biological pump in a one-dimensional ocean model, ,

445 27(February), 1–14, doi:10.1002/gbc.20031, 2013.
446 Bienfang, P.: SETCOL - A technologically simple and reliable method for measuring
447 phtoplankton sinking rates, Can. J. Fish. Aquat. Sci., 38(10), 1289–1294, 1981.
448 Boyd, P. and Trull, T.: Understanding the export of biogenic particles in oceanic waters: Is
449 there consensus?, Prog. Oceanogr., 72(4), 276–312, doi:doi:10.1016/j.pocean.2006.10.007,
450 2007.
451 Buesseler, K. and Boyd, P.: Shedding light on processes that control particle export and flux
452 attenuation in the twilight zone of the open ocean, Limnol. Oceanogr., 54(4), 1210–1232,
453 2009.
454 Buesseler, K., Antia, A. N., Chen, M., Fowler, S. W., Gardner, W. D., Gustafsson, O.,
455 Harada, K., Michaels, A. F., van der Loeff'o, M. R., Sarin, M., Steinberg, D. K. and Trull, T.:
456 An assessment of the use of sediment traps for estimating upper ocean particle fluxes, J. Mar.
457 Res., 65(3), 345–416, 2007.
458 Cavan, E. L., Le Moigne, F. A. C., Poulton, A. J., Tarling, G. A., Ward, P., Daniels, C. J.,
459 Fragoso, G. M. and Sanders, R. J.: Attenuation of particulate organic carbon flux in the
460 Scotia Sea, Southern Ocean, is controlled by zooplankton fecal pellets, Geophys. Res. Lett.,
461 42(3), 821–830, 2015.
462 Dall'Olmo, G., Dingle, J., Polimene, L., Brewin, R. J. W. and Claustre, H.: Substantial
463 energy input to the mesopelagic ecosystem from the seasonal mixed-layer pump, Nat. Geosci,
464 9(11), 820–823 [online] Available from: http://dx.doi.org/10.1038/ngeo2818, 2016.
465 Devol, A. H. and Hartnett, H. E.: Role of the oxygen-deficient zone in transfer of organic
466 carbon to the deep ocean, Limnol. Oceanogr., 46(7), 1684–1690,
467 doi:10.4319/lo.2001.46.7.1684, 2001.
468 Ebersbach, F. and Trull, T. W.: Sinking particle properties from polyacrylamide gels during
469 the KErguelen Ocean and Plateau compared Study (KEOPS): Zooplankton control of carbon

export in an area of persistent natural iron inputs in the Southern Ocean, Limnol. Oceanogr., 53(1), 212–224, doi:10.4319/lo.2008.53.1.0212, 2008.

Francois, R., Honjo, S., Krishfield, R. and Manganini, S.: Factors controlling the flux of organic carbon to the bathypelagic zone of the ocean, Global Biogeochem. Cycles, 16(4), 34–1–34–20, doi:10.1029/2001GB001722, 2002.

François, R., Honjo, S., Krishfield, R. and Manganini, S.: Factors controlling the flux of organic carbon to the bathypelagic zone of the ocean, Global Biogeochem. Cycles, 16(4), 1087, doi:doi:10.1029/2001GB001722, 2002, 2002.

Guidi, L., Stemmann, L., Legendre, L., Picheral, M., Prieur, L. and Gorsky, G.: Vertical distribution of aggregates (>110 μm) and mesoscale activity in the northeastern Atlantic: Effects on the deep vertical export of surface carbon, Limnol. Oceanogr., 52(1), 7–18, doi:10.4319/lo.2007.52.1.0007, 2007.

Hansen, A. N. and Visser, A. W.: Carbon export by vertically migrating zooplankton: an adaptive behaviour model., Prepr. Submitt. to Mar. Ecol. Prog. Ser., doi:10.1002/lno.10249, 2016.

Hartnett, H. E., Devol, A. H., Keil, R. G., Hedges, J. and Devol, A. H.: Influence of oxygen exposure time on organic carbon preservation in continetal margin sediments, Nature, 391(February), 2–4, 1998.

Henson, S., Sanders, R. and Madsen, E.: Global patterns in efficiency of particulate organic carbon export and transfer to the deep ocean, Global Biogeochem. Cycles, 26(1028), 14, doi:doi:10.1029/2011GB004099, 2012.

Henson, S., Yool, A. and Sanders, R.: Variability in efficiency of particulate organic carbon export: A model study, Global Biogeochem. Cycles, 33–45, doi:10.1002/2014GB004965.Received, 2015.

Herndl, G. and Reinthaler, T.: Microbial control of the dark end of the biological pump., Nat.

Geosci., 6(9), 718–724, doi:10.1038/ngeo1921, 2013.

Hilting, A. K., Kump, L. R. and Bralower, T. J.: Variations in the oceanic vertical carbon isotope gradient and their implications for the Paleocene-Eocene biological pump, Paleoceanography, 23(3), PA3222, doi:10.1029/2007PA001458, 2008.

Keil, R. G., Neibauer, J., Biladeau, C., van der Elst, K. and Devol, A. H.: A multiproxy approach to understanding the "enhanced" flux of organic matter through the oxygen deficient waters of the Arabian Sea, Biogeosciences, 13, 2077–2092, doi:10.5194/bgd-12-17051-2015, 2016.

Kwon, E., Primeau, F. and Sarmiento, J.: The impact of remineralization depth on the air-sea carbon balance, Nat. Geosci., 2, 630–635, 2009.

De La Rocha, C. and Passow, U.: Factors influencing the sinking of POC and the efficiency of the biological carbon pump, Deep Sea Res. Part II Top. Stud. Oceanogr., 54(5-7), 639–658, doi:10.1016/j.dsr2.2007.01.004, 2007.

Lam, P. J., Doney, S. C. and Bishop, J. K. B.: The dynamic ocean biological pump: insights from a global compilation of Particulate Organic Carbon, CaCO3 and opal concentrations profiles from the mesopelagic., Global Biogeochem. Cycles, doi:doi:10.1029/2010GB003868, 2011.

Lampitt, R., Noji, T. and Bodungen, B.: What happens to zooplankton faecal pellets? Implications for vertical flux, Mar. Biol., 23, 15–23, 1990.

Lampitt, R., Bett, B., Kiriakoulakis, K., Popova, E., Ragueneau, O., Vangriesheim, A. and Wolff, G. A.: Material supply to the abyssal seafloor in the Northeast Atlantic, Prog. Oceanogr., 50(1-4), 27–63, 2001.

Lampitt, R. S., Boorman, B., Brown, L., Lucas, M., Salter, I., Sanders, R., Saw, K., Seeyave, S., Thomalla, S. J. and Turnewitsch, R.: Particle export from the euphotic zone: Estimates using a novel drifting sediment trap, Th-234 and new production, Deep. Res. Part I-

520 Oceanographic Res. Pap., 55(11), 1484–1502, doi:DOI 10.1016/j.dsr.2008.07.002, 2008.
521 Laurenceau, E., Trull, T. W., Davies, D. M., Bray, S. G., Doran, J., Planchon, F. and Carlotti,
522 F.: The relative importance of phytoplankton aggregates and zooplankton fecal pellets to
523 carbon export : insights from free-drifting sediment trap deployments in naturally iron-
524 fertilised waters near the Kerguelen Plateau, , 1007–1027, doi:10.5194/bg-12-1007-2015,
525 2015.
526 Laws, E., Falkowski, P. G., Smith, W. O., Ducklow, H. and McCarthy, J. J.: Temperature
527 effects on export production in the open ocean, Global Biogeochem. Cycles, 14(4), 1231–
528 1246 [online] Available from: <Go to ISI>://000166341000019, 2000.
529 Maiti, K., Charette, M. a., Buesseler, K. O. and Kahru, M.: An inverse relationship between
530 production and export efficiency in the Southern Ocean, Geophys. Res. Lett., 40(November
531 2012), doi:10.1002/grl.50219, 2013.
532 Manno, C., Stowasser, G., Enderlein, P., Fielding, S. and Tarling, G. A.: The contribution of
533 zooplankton faecal pellets to deep-carbon transport in the Scotia Sea (Southern Ocean),
534 Biogeosciences, 12(6), 1955–1965, doi:10.5194/bg-12-1955-2015, 2015.
535 Marsay, C., Sanders, R., Henson, S., Pabortsava, K., Achterberg, E. and Lampitt, R.:
536 Attenuation of sinking particulate organic carbon flux through the mesopelagic ocean, Proc.
537 Natl. Acad. Sci., 12(4), 1089–1094, 2015.
538 Martin, J., Knauler, G., Karl, D. and Broenkow, W.: VERTEX: carbon cycling in the north
539 east Pacific, Deep. Res., 34(2), 267–285, 1987a.
540 Martin, J. H.: Glacial-interglacial CO/sub 2/ change: the iron hypothesis,
541 Paleoceanography|Paleoceanography, 5(1), 1–13 [online] Available from: <Go to
542 ISI>://INSPEC:3655190, 1990.
543 Martin, J. H., Knauer, G. A., Karl, D. M. and Broenkow, W. W.: Vertex - Carbon Cycling in
544 the Northeast Pacific, Deep. Res. Part A, 34(2), 267–285 [online] Available from: <Go to

ISI>://A1987G837500008, 1987b.

Mayor, D. J., Sanders, R., Giering, S. L. C. and Anderson, T. R.: Microbial gardening in the ocean's twilight zone, Bioessays, 36(12), 1132–7, doi:10.1002/bies.201400100, 2014.

Le Moigne, F. A. C., Henson, S. A., Cavan, E., Georges, C., Pabortsava, K., Achterberg, E. P., Ceballos-Romero, E., Zubkov, M. and Sanders, R. J.: What causes the inverse relationship between primary production and export efficiency in the Southern Ocean?, Geophys. Res. Lett., doi:10.1002/2016GL068480, 2016.

Le Moigne, F., Sanders, R., Villa-Alfageme, M., Martin, A. P., Pabortsava, K., Planquette, H., Morris, P. and Thomalla, S.: On the proportion of ballast versus non-ballast associated carbon export in the surface ocean, Geophys. Res. Lett., 39(15), doi:10.1029/2012GL052980, 2012.

Van Mooy, B. A. S., Keil, R. G. and Devol, A. H.: Impact of suboxia on sinking particulate organic carbon : Enhanced carbon flux and preferential degradation of amino acids via denitrification, Geochim. Cosmochim. Acta, 66(3), 457–465, 2002.

Parekh, P., Dutkiewicz, S., Follows, M. J. and Ito, T.: Atmospheric carbon dioxide in a less dusty world, Geophys. Res. Lett., 33, doi:doi:10.1029/2005GL025098, 2006.

Park, J., Oh, I.-S., Kim, H.-C. and Yoo, S.: Variability of SeaWiFs chlorophyll-a in the southwest Atlantic sector of the Southern Ocean: Strong topographic effects and weak seasonality, Deep Sea Res. Part I Oceanogr. Res. Pap., 57(4), 604–620, doi:10.1016/j.dsr.2010.01.004, 2010.

Paulmier, A. and Ruiz-Pino, D.: Oxygen minimum zones (OMZs) in the modern ocean, Prog. Oceanogr., 80(3-4), 113–128, doi:10.1016/j.pocean.2008.08.001, 2009.

Pollard, R. T., Salter, I., Sanders, R. J., Lucas, M. I., Moore, C. M., Mills, R. A., Statham, P. J., Allen, J. T., Baker, A. R., Bakker, D. C. E., Charette, M. A., Fielding, S., Fones, G. R., French, M., Hickman, A. E., Holland, R. J., Hughes, J. A., Jickells, T. D., Lampitt, R. S.,

570 Morris, P. J., Nedelec, F. H., Nielsdottir, M., Planquette, H., Popova, E. E., Poulton, A. J.,
571 Read, J. F., Seeyave, S., Smith, T., Stinchcombe, M., Taylor, S., Thomalla, S., Venables, H.
572 J., Williamson, R. and Zubkov, M. V: Southern Ocean deep-water carbon export enhanced by
573 natural iron fertilization, Nature, 457(7229), 577–U81, doi:Doi 10.1038/Nature07716, 2009.
574 Puigcorbé, V., Benitez-Nelson, C. R., Masqué, P., Verdeny, E., White, A. E., Popp, B. N.,
575 Prahl, F. G. and Lam, P. J.: Small phytoplankton drive high summertime carbon and nutrient
576 export in the Gulf of California and Eastern Tropical North Pacific, Global Biogeochem.
577 Cycles, 29(8), 1309–1332, doi:10.1002/2015GB005134, 2015.
578 Redfield, A. C.: On the proportions of organic derivatives in sea water and their relation to
579 the composition of plankton, University Press of Liverpool., 1934.
580 Riley, J., Sanders, R., Marsay, C., Le Moigne, F., Achterberg, E. and Poulton, A.: The
581 relative contribution of fast and slow sinking particles to ocean carbon export, Global
582 Biogeochem. Cycles, 26, doi:doi:10.1029/2011GB004085, 2012.
583 Romero-Ibarra, N. and Silverberg, N.: The contribution of various types of settling particles
584 to the flux of organic carbon in the Gulf of St. Lawrence, Cont. Shelf Res., 31(16), 1761–
585 1776, doi:10.1016/j.csr.2011.08.006, 2011.
586 Salter, I., Lampitt, R. S., Sanders, R., Poulton, A., Kemp, A. E. S., Boorman, B., Saw, K. and
587 Pearce, R.: Estimating carbon, silica and diatom export from a naturally fertilised
588 phytoplankton bloom in the Southern Ocean using PELAGRA: A novel drifting sediment
589 trap, Deep. Res. Part Ii-Topical Stud. Oceanogr., 54(18-20), 2233–2259,
590 doi:10.1016/j.dsr2.2007.06.008, 2007.
591 Sanders, R., Henson, S. A., Koski, M., De La Rocha, C. L., Painter, S. C., Poulton, A. J.,
592 Riley, J., Salihoglu, B., Visser, A., Yool, A., Bellerby, R. and Martin, A. P.: The Biological
593 Carbon Pump in the North Atlantic, Prog. Oceanogr., 129, 200–218,
594 doi:10.1016/j.pocean.2014.05.005, 2014.

595 Smythe-Wright, D., Boswell, S., Kim, Y.-N. and Kemp, A.: Spatio-temporal changes in the
596 distribution of phytopigments and phytoplanktonic groups at the Porcupine Abyssal Plain
597 (PAP) site, Deep Sea Res. Part II Top. Stud. Oceanogr., 57(15), 1324–1335,
598 doi:10.1016/j.dsr2.2010.01.009, 2010.
599 Takahashi, T., Sutherland, S., Sweeney, C., Poisson, A., Metzl, N., Tilbrook, B., Bates, N.,
600 Wanninkhof, R., Feely, R., Sabine, C., Olafsson, J. and Nojiri, Y.: Global sea–air CO2 flux
601 based on climatological surface ocean pCO2, and seasonal biological and temperature effects,
602 Deep Sea Res. Part II Top. Stud. Oceanogr., 49(9-10), 1601–1622, doi:10.1016/S0967-
603 0645(02)00003-6, 2002.
604 Tarling, G. A., Shreeve, R., Ward, P. and Hirst, A.: Life-cycle phenotypic composition and
605 mortality of Calanoides actus in the Scotia Sea; a modeling approach, Mar. Ecol. Prog. Ser.,
606 272, 165–181, 2004.
607 Williams, R. L., Wakeham, S., McKinney, R. and Wishner, K. F.: Trophic ecology and
608 vertical patterns of carbon and nitrogen stable isotopes in zooplankton from oxygen
609 minimum zone regions, Deep. Res. Part I Oceanogr. Res. Pap., 90(1), 36–47,
610 doi:10.1016/j.dsr.2014.04.008, 2014.
611 Wilson, S., Steinberg, D. and Buesseler, K.: Changes in fecal pellet characteristics with depth
612 as indicators of zooplankton repackaging of particles in the mesopelagic zone of the
613 subtropical and subarctic North Pacific Ocean, Deep. Res. Part Ii-Topical Stud. Oceanogr.,
614 55(14-15), 1636–1647, doi:10.1016/j.dsr2.2008.04.019, 2008.
615 Wilson, S., Ruhl, H. and Smith, K.: Zooplankton fecal pellet flux in the abyssal northeast
616 Pacific : A 15 year time-series study, Limnol. Oceanogr., 58(3), 881–892,
617 doi:10.4319/lo.2013.58.3.0881, 2013.
618 Wishner, K. F., Outram, D. M., Seibel, B. A., Daly, K. L. and Williams, R. L.: Zooplankton
619 in the eastern tropical north Pacific: Boundary effects of oxygen minimum zone expansion,

620 Deep Sea Res. Part I Oceanogr. Res. Pap., 79, 122–140, doi:10.1016/j.dsr.2013.05.012, 2013.
621 Yool, A., Popova, E. E. and Anderson, T. R.: MEDUSA-2.0: an intermediate complexity
622 biogeochemical model of the marine carbon cycle for climate change and ocean acidification
623 studies, Geosci. Model Dev., 6(5), 1767–1811, doi:10.5194/gmd-6-1767-2013, 2013.
624

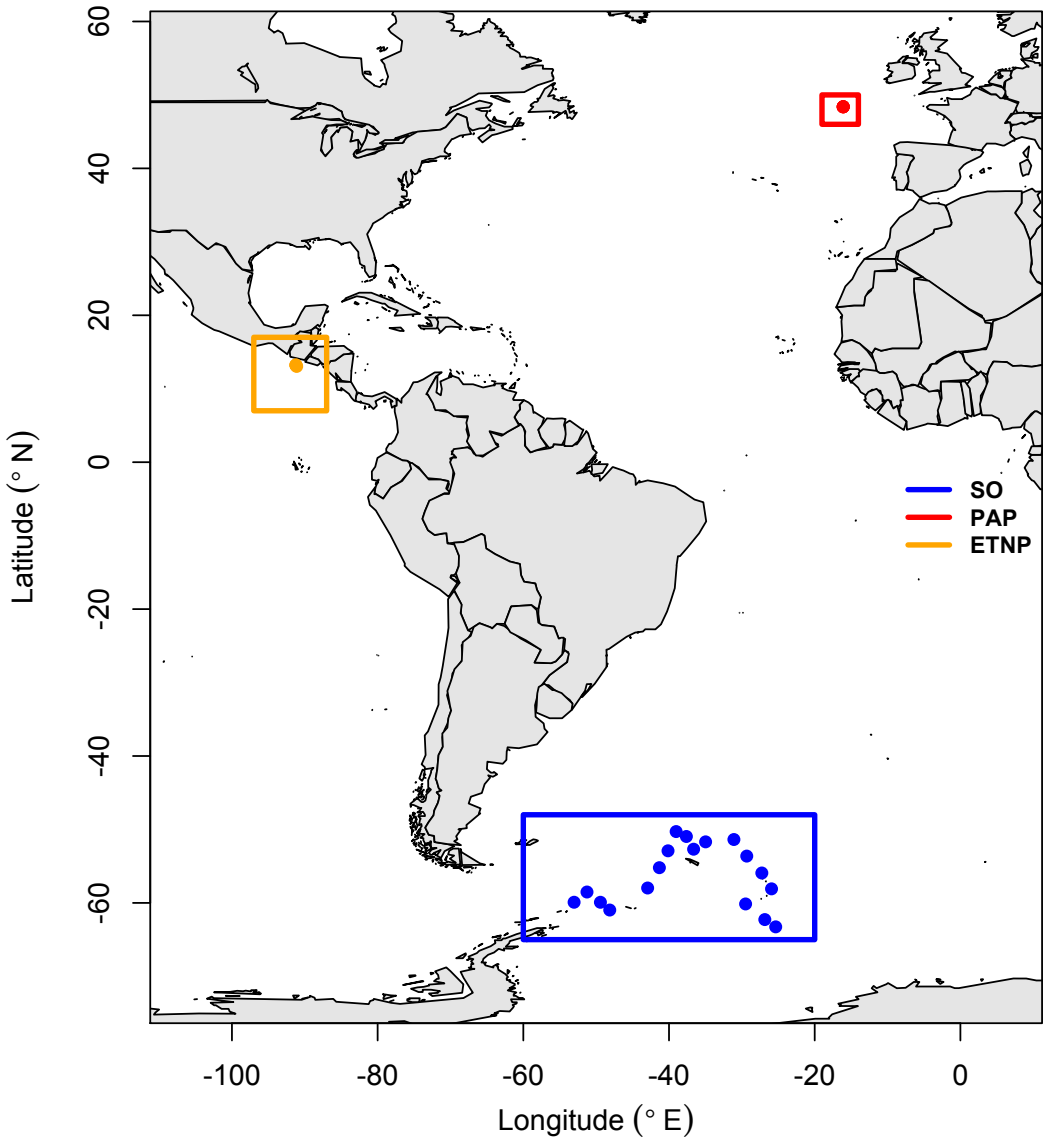

625

626 **Fig. 1.** Map showing study areas. Blue rectangle is location of sites in the Southern Ocean,

627 red is the North Atlantic Porcupine Abyssal Plain and orange the equatorial north Pacific

628 oxygen minimum zone.

629

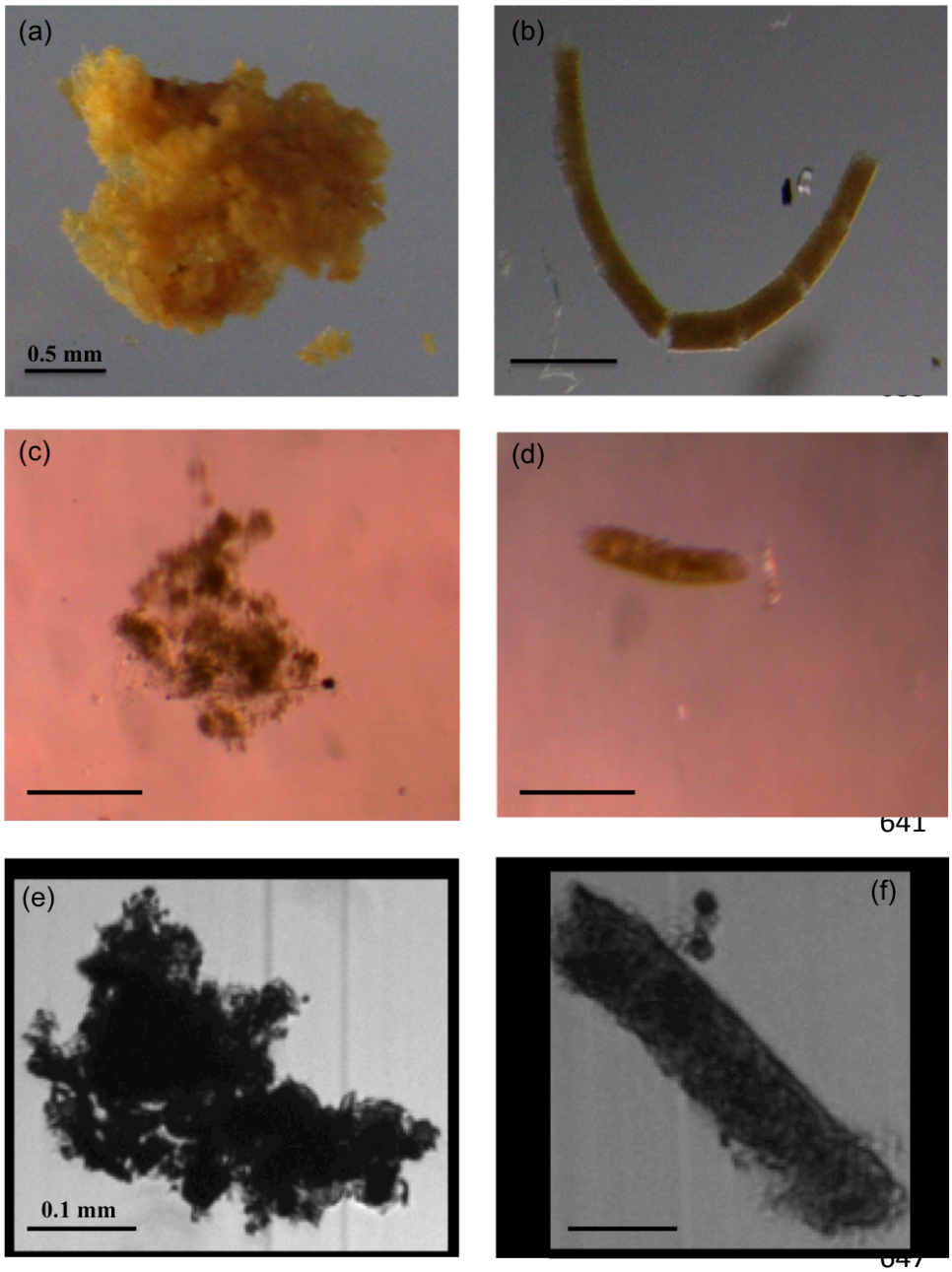

Fig. 2. Particle images from the 3 different regions; Southern Ocean (a & b), PAP site (c & d) and the ETNP (e & f). a, c & e are phytodetrital aggregates and b, d & f are faecal pellets. b is a chain of krill pellets from the SO and d & f are copepod pellets. Scale bars are 0.5 mm for the SO and PAP images (a-d) and 0.1 mm for the ETNP (e & f). A stereomicroscope was used in the SO, a compound microscope at PAP and a FlowCAM in the ETNP, giving rise to the different background colours and shades.

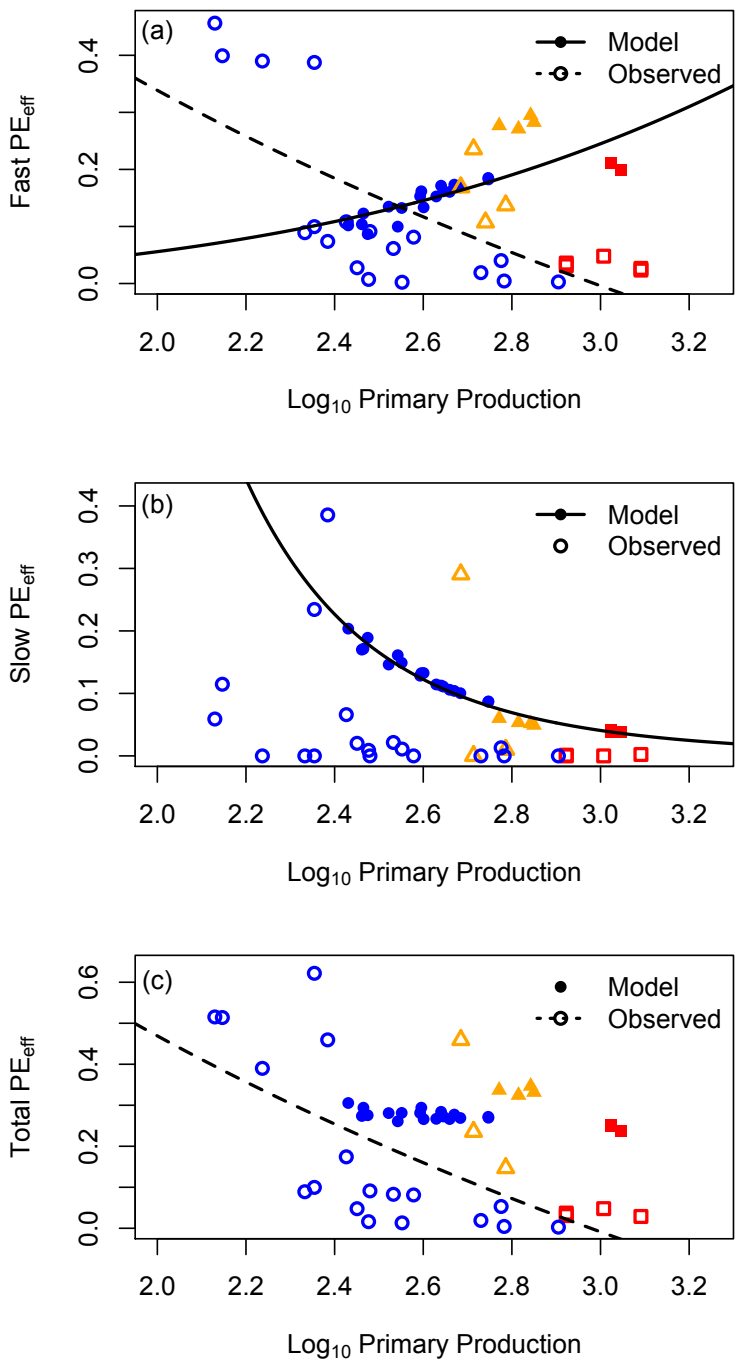

Fig. 3. Primary production against particle export efficiency (PE*eff*) for (a) fast sinking, (b) slow sinking and (c) total sinking particles. Blue circles are Southern Ocean, red squares PAP and orange triangles equatorial Pacific. Filled circles and solid black lines show model output and open circles and dashed lines are observations. All fitted lines are statistically significant to at least the 95 % level (see text for details).

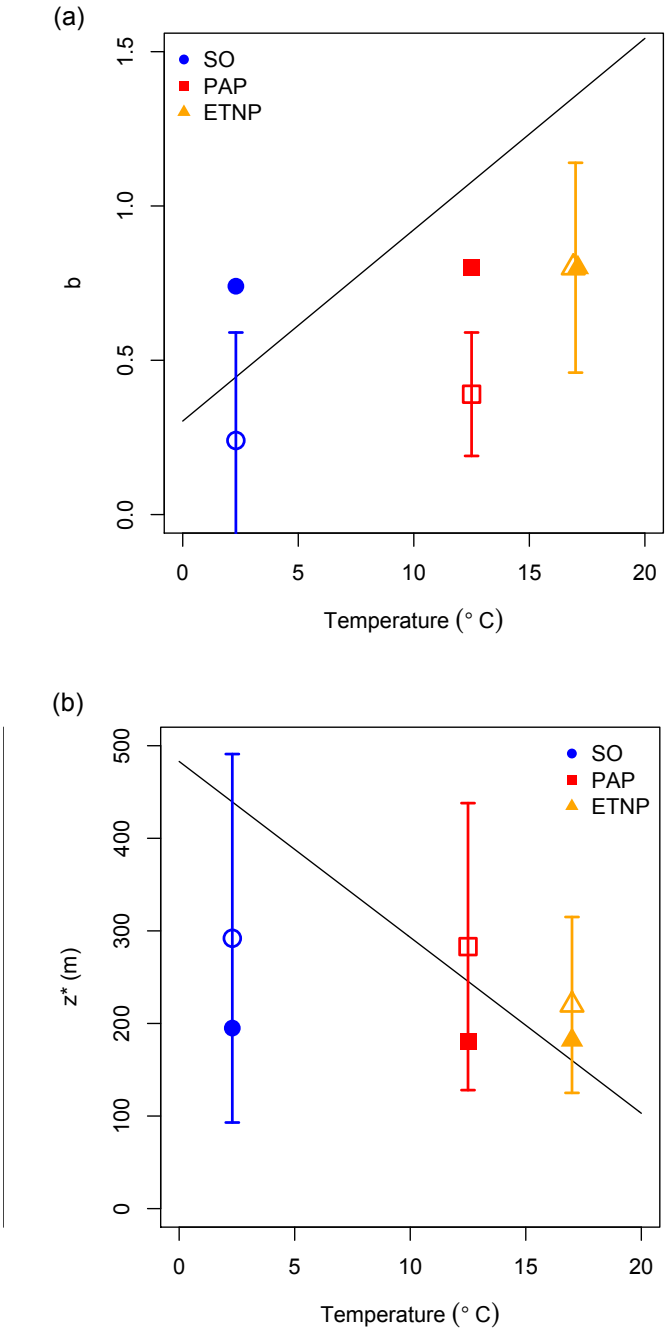

Fig. 4. Total sinking POC attenuation coefficients (a) *b* and (b) *z** with temperature. Blue circles are Southern Ocean, red squares PAP and orange triangles equatorial Pacific. Filled points show model output and open points are observations. Solid line is Marsay et al. (2015) regression. Error bars are standard error of the mean and only plotted on the observations as the error is too small in the model. See Table S2 for attenuation coefficients of fast and slow sinking particles.

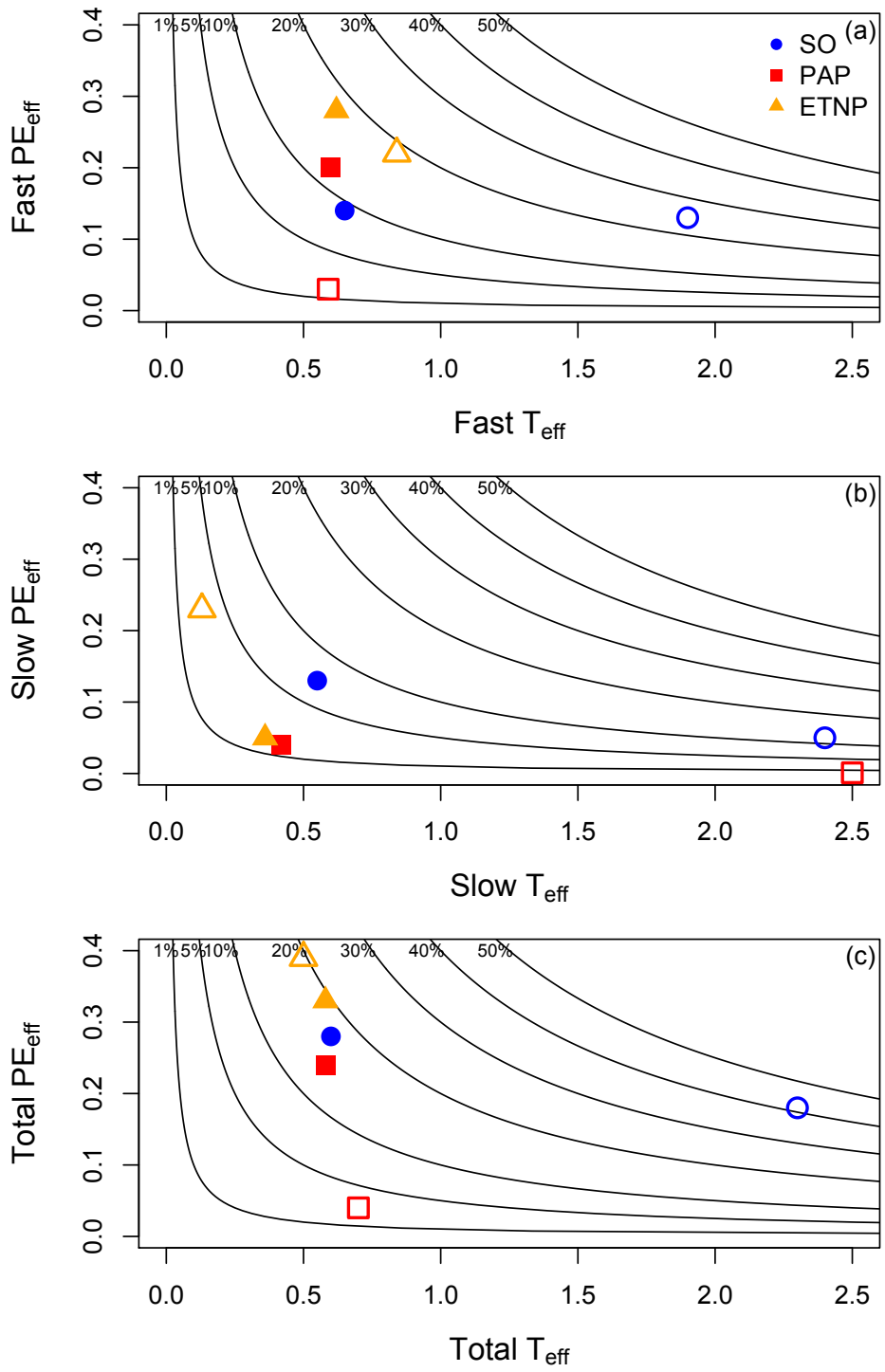

Fig. 5. Efficiency of the biological carbon pump for (a) fast, (b) slow and (c) total sinking particles. Particle export efficiency (PE*eff*) is plotted against transfer efficiency (T*eff*). Contours represent BCP*eff* (proportion of primary production reaching depths of 150-300 m). Blue circles are Southern Ocean, red squares PAP and orange triangles equatorial Pacific. Filled points show model output and open points are observations.